AVOIDING LOCAL MINIMA IN ENTROPY-BASED SAR AUTOFOCUS

Robert L. Morrison, Jr., David C. Munson, Jr., and Minh N. Do

Coordinated Science Laboratory
Dept. of Electrical and Computer Engineering
University of Illinois at Urbana-Champaign
rlmorris@uiuc.edu, munson@eecs.umich.edu, minhdo@uiuc.edu

ABSTRACT

This paper explores the problem of avoiding local minima solutions in entropy-based synthetic aperture radar (SAR) autofocus. These autofocus algorithms correct defocused SAR images by determining the phase error estimate that produces the image with minimum entropy. However, the optimization strategy may converge to local minima solutions that correspond to incorrect image restorations. We propose two methods for reducing the likelihood of achieving such solutions. The first is a novel wavelet-based decomposition technique that determines the neighborhood of the global entropy minimum. A second strategy is the application of simulated annealing techniques to the optimization. We explore the performance of these methods using simulated SAR data, and provide a justification for how they work. Worst case phase errors in which the phase is random and uncorrelated between elements are considered.

1. INTRODUCTION

In SAR, the received Fourier imaging data are typically corrupted by an unknown 1-D phase error function $\phi_e(X)$. The phase error results in a 1-D defocusing of the reconstructed image. The corrupted Fourier data $G(X,Y)$ are related to the desired original data $F(X,Y)$ by

$$G(X,Y) = F(X,Y)e^{j\phi_e(X)}, \tag{1}$$

where X and Y are spatial frequency variables. Autofocus algorithms create an estimate of the phase error function $\hat{\phi}_e(X)$ to form the corrected Fourier data $\hat{F}(X,Y)$. A recent approach to SAR autofocus involves the use of entropy as a cost metric for image focus. The phase error estimate is selected to minimize the entropy of the image. SAR images tend to consist of bright pointlike features against a clutter background. When images of this type are considered, the minimum entropy image is found to be in excellent agreement with the original [1]. Throughout this paper, we will use E to denote entropy, with entropy defined as in [3].

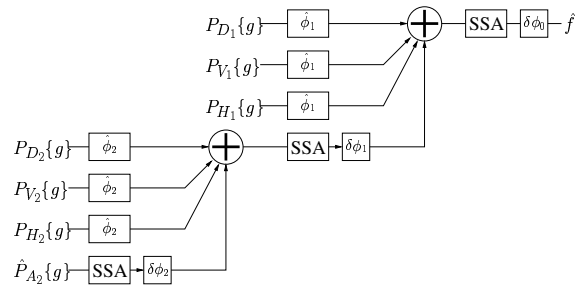

Fig. 1. Diagram of wavelet-based technique.

In this paper, we consider the Stage By Stage Approaching (SSA) optimization algorithm for determining the entropy minimum, which performs a coordinate direction search for each phase element [3]. This technique is of interest because it is conceptually simple, easily implemented, and does not require the computation of a function gradient. In addition, SSA can outperform the standard phase gradient autofocus (PGA) in restoration quality [1]. However, this approach can be problematic because the algorithm can only search downhill; autofocus parameters are always updated in the direction that decreases the cost metric. Thus, there is the likelihood of the algorithm becoming trapped in a local minimum, and not converging to the correct global minimum. In practice, we observe that the likelihood of local minima solutions increases as the signal-to-clutter ratio of the underlying image decreases. We have analytically demonstrated that the entropy surface $E(\phi(X))$ resulting from the simplest image model, a single unit impulse without clutter, contains local minima. We have conducted work aimed at reducing the probability of convergence to local minima. Promising results have been achieved using a novel wavelet-based decomposition method, and also using the ideas of simulated annealing.

2. WAVELET-BASED ENHANCEMENT

Our wavelet-based technique is motivated by the observation that when the corrupt image is projected onto a smooth subspace, most of the (defocused) signal content is retained and the clutter is decreased. In a coarse (low resolution) smooth subspace, the global properties of the entropy surface are preserved, while local minima resulting from clutter are reduced. Thus, performing autofocus processing in this space yields a phase estimate in the neighborhood of the actual global minimum. Using this phase estimate as a starting point, and applying the autofocus routine to a higher resolution smooth subspace, a solution closer to the global minimum is obtained. This process repeats recursively using increasingly finer spaces until the full-resolution image is reached, at which point the phase error estimate has converged to the desired global entropy minimum.

Figure 1 shows a block diagram of the wavelet decomposition scheme, where P is the projection operator and the subscripts indicate diagonal, vertical, horizontal, and approximation subspaces. Two levels of decomposition are depicted in the figure. Using Mallat's algorithm extended to two dimensions, we first determine the projections of the corrupt image onto the detail and approximation subspaces up to level J. The wavelet-based decomposition repeats recursively; the algorithm progresses from level j to level $j-1$ until the size of the full scale image is reached. The projection onto the next level in approximation space (level $j-1$) is formed by the sum of the projections from the previous level:

$$P_{A_{j-1}}\{g\} = P_{A_j}\{g\} + P_{D_j}\{g\} + P_{V_j}\{g\} + P_{H_j}\{g\}. \quad (2)$$

The phase error estimate from the previous level j is applied to $P_{A_{j-1}}\{g\}$ to form the focused projection $\hat{P}_{A_{j-1}}\{g\}$. This relationship is expressed in the Fourier domain as

$$\hat{\rho}_{A_{j-1}}\{g\} = \rho_{A_{j-1}}\{g\} \cdot e^{-j\hat{\phi}_j(X)}, \quad (3)$$

where $\rho_{A_j}\{g\} = DFT_{x,y}[P_{A_j}\{g\}]$. At each level of the decomposition, SSA is applied to the focused projections $\hat{P}_{A_{j-1}}\{g\}$ to produce incremental phase estimates $\delta\phi_{j-1}$. The phase error estimate at level j can be expressed as a summation of the incremental phase estimates, starting with the initial estimate from the coarsest level J:

$$\hat{\phi}_j = \sum_{k=j}^{J} \delta\phi_k. \quad (4)$$

Using (4), the focused projection at level $j-1$ is related to the focused projection at the previous level by

$$\hat{\rho}_{A_{j-1}}\{g\} = (\rho_{D_j}\{g\} + \rho_{V_j}\{g\} + \rho_{H_j}\{g\})e^{-j\hat{\phi}_j(X)} + \hat{\rho}_{A_j}\{g\}e^{-j\delta\phi_j}. \quad (5)$$

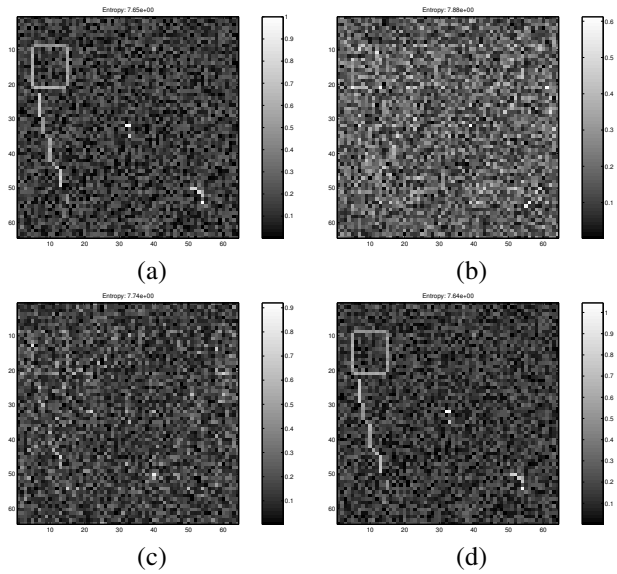

Fig. 2. Synthesized terrain image with increased background clutter: (a) original image (E = 7.65), (b) corrupted image (E = 7.88), (c) reconstruction with standard SSA (E = 7.74), and (d) reconstruction with wavelet variation of SSA (E = 7.64).

The relationship expressed in (5) is seen in the block diagram of Figure 1. It is important to note that the autofocus processing in the wavelet decomposition scheme is equivalent to applying the phase error estimate $\hat{\phi}_0$ to the corrupt image.

To demonstrate the performance of our method, we consider a complex-valued simulated SAR terrain image. The magnitude of this image is displayed in Figure 2(a). The defocused image of Figure 2(b) is formed by applying a white phase error function $\phi_e(X)$, where each element of the phase error is $i.i.d.$ and $U \sim (-\pi, \pi)$, in the Fourier domain. Figure 2(c) indicates that SSA alone is unable to correctly focus the image. The entropies of the original, corrupt, and SSA restored images are 7.65, 7.88, and 7.74, respectively. Figure 2(d) is a restoration formed using SSA with a 1-level Haar decomposition. The wavelet-enhanced method correctly focuses the image. The entropy of the wavelet restoration is 7.64, indicating that standard SSA gets trapped in a local minimum.

It is difficult to establish intuition about the wavelet enhancement method using the complicated image of Figure 2(a). Therefore, we have developed a simple image, shown in Figure 3(a), to demonstrate that our method enables improved focusing by retaining signal content and rejecting clutter. On line 40 of the image, we have introduced a clutter disturbance at pixels 30 and 31 consisting of two adjacent impulses with magnitude 0.5 and a π radian shift be-

tween the two. This clutter disturbance can be considered the simplest representation of the clutter found in SAR images. The ramp structures, and point target on line 45, represent the signal content. The corrupted image of Figure 3(b) is formed by applying a quadratic phase error function. When the clutter disturbance is removed, SSA is able to correctly focus the image. However, with the disturbance in place, SSA cannot restore the image, as demonstrated in Figure 3(c). Figure 3(d) demonstrates that the Haar wavelet decomposition scheme allows the image to be correctly focused.

By the linearity of the wavelet transform, the projections of the corrupt image onto the approximation and detail spaces for the ramp feature and clutter disturbance on line 40 can be considered separately:

$$W[g(x)] = W[b(x) \otimes f_s(x)] + W[b(x) \otimes f_c(x)], \quad (6)$$

where $W[\cdot]$ denotes the wavelet transform, $\otimes$ denotes N-point circular convolution, $b(x)$ is the blurring kernel induced by the Fourier phase error, and $f_s(x)$ and $f_c(x)$ are the ramp (signal) and clutter disturbance, respectively. We have observed that the defocused ramp feature (signal) lies mostly in the approximation space, while the disturbance is primarily in the detail space.

Since the blurring kernel acts only along the rows of the image, it can be beneficial to perform 1-D wavelet decompositions for each row instead of using the 2-D algorithm. Under this scheme, the corrupt image is projected onto one approximation and one detail space (as opposed to the three detail spaces considered in the 2-D case). Improved performance has been observed in some scenarios using the 1-D algorithm in place of the 2-D. We have found decomposition with a Daubechies-2 wavelet to be successful in the 1-D case, but not in 2-D. For the case of the Haar wavelet in 2-D, $2^J - 1$ out of every 2^J rows are redundant. This suggests that the entropy computation can be reduced in the 2-D algorithm by eliminating the redundant rows.

3. SIMULATED ANNEALING SEARCH TECHNIQUE

It is beneficial to occasionally make uphill moves when searching for the entropy minimum so that the autofocus algorithm may escape local minima. Using ideas adapted from *simulated annealing* optimization theory [2], we propose a modification to the SSA search strategy that enables the algorithm to take uphill steps with a small probability. We have achieved promising results using an original simulated annealing-based variation of the SSA search strategy. In SSA, three candidate phase perturbations are computed after each image update; the algorithm may take a positive or negative step, or no step. In our implementation, only one candidate phase perturbation is considered. The candidate

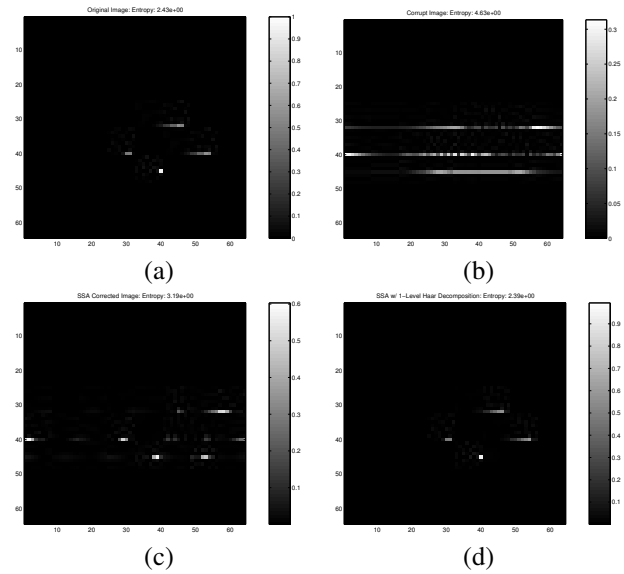

Fig. 3. Simple image with noise disturbance at pixels (40,30) and (40,31): (a) original image (E = 2.43), (b) corrupt image (E = 4.63), (c) restoration with standard SSA (E = 3.19), and (d) restoration using SSA with 1-Level Haar decomposition (E = 2.39).

is either a positive or negative step, and is selected with an equal probability. The step size μ is fixed throughout the entire algorithm, in contrast to standard SSA which decreases μ by a factor of two with each iteration. We chose a value of $\mu = \frac{\pi}{8}$ in our implementation. If the change in entropy with respect to the last perturbation is negative, indicating downhill motion, the candidate is accepted with probability one. If the entropy difference is positive, causing an uphill move, then the candidate is accepted if a random variable uniformly distributed between 0 and 1 falls below a variable threshold. The threshold is a function of the change in entropy ΔE and a "temperature" parameter T that decreases throughout the algorithm. The notion of temperature arises from an analogy with the natural annealing process in which matter is cooled slowly to place it in its lowest energy state; if the temperature were cooled rapidly, the substance would reach a higher energy local minima state. The threshold can be expressed as:

$$\tau(\Delta E, T) = e^{-\frac{\Delta E}{T}}. \quad (7)$$

The choice of an initial value for T varies with the image under consideration. A good rule is to initialize T to be larger than the greatest change in entropy that would occur for a single perturbation using the standard SSA algorithm. The temperature is held constant over a fixed number of cycles, where in each cycle all the phase elements are perturbed. The temperature is then decreased by a particular factor. In

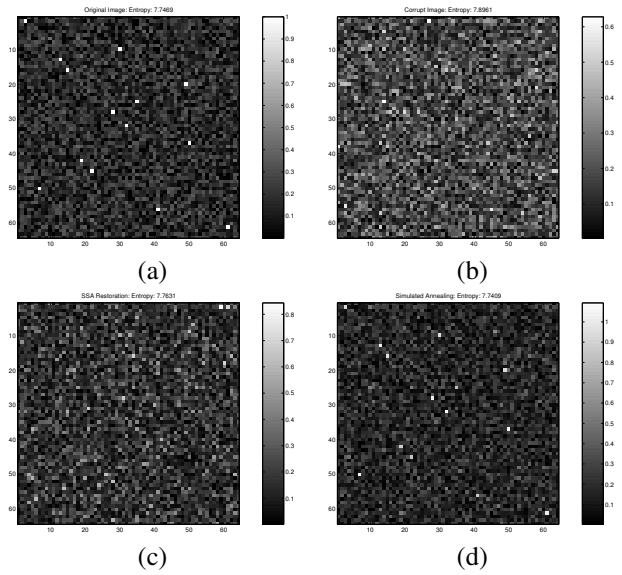

Fig. 4. Synthesized point image: (a) original image (E = 7.7469), (b) corrupted image (E = 7.8961), (c) restoration with standard SSA (E = 7.7631), and (d) restoration with simulated annealing variation of SSA (E = 7.7409).

our implementation, we selected 10 temperature steps, with a 10 percent decrease in temperature at each step, and 25 iterations (cycles) per temperature.

Figure 4 shows a case in which the standard SSA algorithm is unable to restore a particular corrupted (synthetic) image. The simulated annealing variation produces an accurate restoration. Depending on the type of image considered, the simulated annealing algorithm may not always produce a correct restoration. If the signal content of the image is low with respect to surrounding clutter, or it does not contain the pointlike features representative of a SAR image, then the desired solution may not lie in the global minima of the entropy function. However, our simulated annealing algorithm consistently achieves its objective of determining lower entropy states. Figure 5 shows a plot of the restored image entropy for 20 trials of the simulated annealing algorithm using the point image of Figure 4. The entropy of the SSA restoration is displayed as a dashed line for comparison. The figure reveals that in every trial the simulated annealing algorithm produces a lower entropy restoration than SSA.

The simulated annealing algorithm faces the obvious drawback of increased computational expense. We are currently investigating the use of other optimization techniques, such as gradient descent methods, to determine whether similar results can be achieved with increased efficiency.

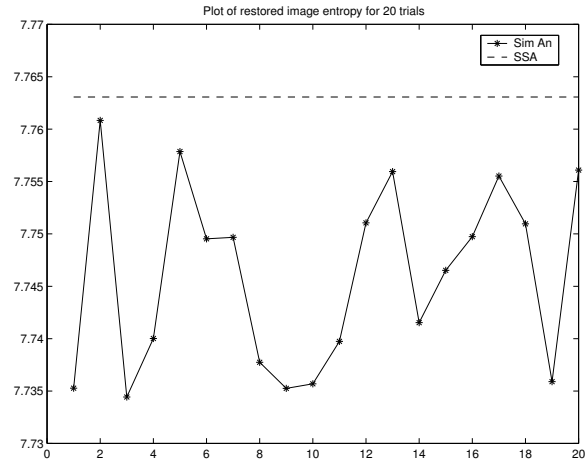

Fig. 5. Restored image entropy for 20 trials of the simulated annealing algorithm. The dashed line is the entropy of the SSA restoration.

4. CONCLUSION

In this paper, we have proposed novel techniques for avoiding local minima solutions in entropy-based SAR autofocus. The first is a wavelet-based method that successively projects the corrupt image onto a series of smooth subspaces. This multiresolution approach allows the global properties of the entropy surface of the image to be inferred so that the algorithm may start its search in the correct "valley" of the global minimum. The second technique involves incorporating the ideas of simulated annealing into the standard SSA search strategy. We have found both approaches to produce superior results in comparison with the existing optimization on a variety of defocused data sets.

5. REFERENCES

[1] R. L. Morrison, Jr. and D. C. Munson, Jr. An experimental study of a new entropy-based SAR autofocus technique. In *Proc. of the IEEE International Conference on Image Processing*, pages 441–444, 2002.

[2] P.J.M. van Laarhoven and E.H.L. Aarts. *Simulated Annealing: Theory and Applications*. D. Reidel Publishing Co., Boston, 1987.

[3] L. Xi, L. Guosui, and J. Ni. Autofocusing of ISAR images based on entropy minimization. *IEEE Transactions on Aerospace and Electronic Systems*, 35(4):1240–1252, October 1999.